Int. J. Morphol.,
41(2):539-547, 2023.

Morphological Effects of Cigarette Smoking on Respiratory System and Related Functions Based on AQPs Expression

Efectos Morfológicos del Consumo de Cigarrillos en el Sistema Respiratorio y Funciones Relacionadas Según la Expresión de AQP

Jinbao Wang[1]; Ruijie Ding[2]; Jiaying Liang[1]; Hui Wang[3] & Pei Wang[1]

WANG, J.; DING, R.; LIANG, J.; WANG, H. & WANG, P. Morphological effects of cigarette smoking on respiratory system and related functions based on AQPs expression. *Int. J. Morphol., 41(2)*:539-547, 2023.

SUMMARY: A great deal of attention of air pollution on respiratory health is increasing, particularly in relation to haze days. It is that exposure to cigarette smoke augments the toxicity of common air contaminants, thereby increasing the complexity of respiratory diseases. Although there are various mechanisms involved to respiratory diseases caused or worsen by cigarette smoking, in which the role of AQPs in the lung with regard to fluid homeostasis still remains elusive. In this paper, we copied the rat models based on smoke generator, and investigated the morphological changes of mucosa and related functions depending on the balance of lining liquid of alveoli via AQPs expression. Compared with normal group, weak labelling of AQP1 and AQP5 protein abundance were clearly detected in the corresponding part of smoke exposure groups compared with normal group. Hence, it is suggested that the contribution of AQPs in the lung is diminished, thereby causing perturbed balancing between resorptive and secretory fluid homeostasis under cigarette smoking.

KEY WORDS: Respiratory system; Cigarette smoking; Pathomorphology; Aquaporins (AQPs); Fluid homeostasis.

INTRODUCTION

Respiratory system includes the lungs and all levels of tracts that link the site of gas exchange with the external environment. It is divided mainly into upper (from the nasal and oral cavities to the throat) and lower (trachea and lung) systems in mammalian, which are separated by the glottis. Each part has specific function and mainly carries the function of ventilation and oxygenation (namely exchange of O_2 and CO_2 between inspired air and blood) (Sato & Kiyono, 2012). Understandably, the upper respiratory tract is the entrance way for oxygen inhaled in the inspired air, and the mucosal surfaces in this part are more likely exposed to external environmental substances, such as all kinds of chemical materials (e.g. cigarette smoke) and allergen particulates (e.g. pollen and house dust).

Most of the respiratory tract is lined with ciliated pseudostratified columnar epithelium that contain a rich population of goblet cells and is referred as respiratory epithelium, which typically consists of 5 cell types. Ciliated columnar cells with well-developed cilia on the apical surface constitute the most abundant type among epithelial cells. The luminal side of the respiratory tract is physically protected by layers of epithelial cells that are adhered tightly each other at tight junctions (Tsukita *et al*., 2008; Yonemura, 2011). The epithelial cells have well-developed cilia and produce mucus composed primarily of polysaccharides such as mucin. Foreign bodies (e.g. tobacco and dust) that do become trapped in the mucin are carried toward the mouth by ciliary movement and expelled by coughing. This mechanism is called mucociliary clearance (Wanner, 1986). However, small foreign bodies, including most pathogens, can easily escape the physical barrier system and arrive at the pulmonary alveoli by inhalation.

[1] School of Basic Medicine, Ningxia Medical University, Yinchuan, 750004 Ningxia, China.
[2] School of Clinical Medicine, Ningxia Medical University, Yinchuan, 750004 Ningxia, China.
[3] Laboratory Animal Center, Ningxia Medical University, Yinchuan, 750004 Ningxia, China.

This work was supported by the Natural Science Fund of Ningxia (2020AAC03167) and Innovation and Entrepreneurship Training Program for Undergraduates of Ningxia Medical University (S202110752051), China.

Received: 2023-01-20 Accepted: 2023-02-15

Previous studies suggested that it is critical to keep fluid balance in respiratory tract and alveolus to maintain normal respiratory function. When the respiratory tract was insulted, it may bring fluid transport disorders, such as airway and lung edema, pleural effusion, etc. Conversely, if there is extra fluid absorption, the airway may become relatively dry and induce thick sputum and subsequent respiratory tract inflammation (Song *et al*., 2017). Aquaporins (AQPs) are water channel proteins supposed to facilitating fluid transport in airway humidification, submucosal gland secretion and alveolar space (Krane & Goldstein, 2007; Song *et al*., 2017). So far, there are 4 AQPs expressed in the lungs and airways, including AQP1, AQP3, AQP4 and AQP5, and their localization seems to be quite conserved between mice, rat and human. (Nielsen *et al*., 1993; Folkesson *et al*., 1994; Nielsen *et al*., 1997; Funaki *et al*., 1998; Kreda *et al*., 2001; Krane *et al*., 2001).

Air pollution is a pervasive risk factor associated with many diseases, and the respiratory tract is the most likely insulted. It is that exposure to cigarette smoke augments the toxicity of common air contaminants, thereby increasing the complexity of respiratory diseases. However, a full understanding of mechanisms involved to respiratory diseases is still unclear, in particular health effects of air pollutants on mucosa of respiratory tract and related lung functions. In this study, we aimed to copy the rat models based on smoke generator, and to investigate the pathomorphology of mucosa and related functions based on fluid balance in the lungs via AQPs expression, thereby providing potential cross-talk mechanisms between the air pollutions (cigarette smoke) and respiratory diseases.

MATERIAL AND METHOD

Experimental animals and protocols. All experimental procedures and protocols in the study were approved by Animal Ethics Committee of the Ningxia Hui Autonomous Region, China.

Sprague Dawley (SD) rats were obtained from the Laboratory Animal Center, Ningxia Medical University and Ningxia Hui Autonomous Region. To avoid the impact of gender on this experiment, healthy and male SD aged about 8 weeks and weighting about 240 g were used at the beginning of the experiment (n=36). All animals were bred in-house and had free access to clean water and rat chow for the duration of the study. After one week of adaptive feeding, the rats were randomly assigned four groups, a normal group (n=18) and three smoke exposure groups (n=6, respectively). Rats of three exposure groups were respectively exposed to cigarette smoke (DSI/BUXCO-Inhalation Tower, USA) during the daytime for 4 h per day, 5 days per week from May to June (1st month), May to July (2nd month) and May to August 2021 (3rd month). Rats were housed in steel cages in a controlled temperature room at 23±2 ºC, exposed to a daily 12-hour light-dark cycle (lights on at 7:00 a.m. and off at 7:00 p.m.) in the Laboratory Animal Center of Ningxia Medical University, China.

Measurement of lung function indexes. After a month of exposure to cigarette smoke, the body weight of rats in the normal group and 1st month smoke exposure group were recorded. Meanwhile, lung function indexes (e.g. FRC, Functional Residual Capacity; FVC, Forced Vital Capacity; IC, Inspiratory Capacity; PEF, Peak Expiratory Flow; MMEF, Maximal Mid-expiratory Flow; ERV, Expiratory Reserve Volume) were detected by Pulmonary Function Testing (DSI/BUXCO® PFT Controller, USA). The latter two smoke exposure groups followed the same procedures as above.

Electron microscopy. Samples of nasal cavities, trachea and lung were collected. For transmission electron microscopy, fresh specimens, about 1 mm^3 in size, were fixed in 4 % phosphate buffered glutaraldehyde for 2h at 4 ºC. Subsequently, these were immersed in 1 % solution of osmium tetroxide in a phosphate buffered at 4 ºC.The specimens were then dehydrated in ascending grades of ethanol and embedded in Epoxy, and sectioned in ultra-thin slice. Sections were stained with uranyl acetate and observed using transmission electron microscopy (Zeiss, Oberkochen, Germany). For scanning electron microscopy, sample surfaces were sputter coated with gold and examined using scanning electron microscopy with an energy dis-perse spectrometer (SEM-EDS) (Hitachi S-3400N, Hitachi, Chiyoda, Tokyo, Japan).

Immunolight microscopy. Samples were collected and immediately fixed with 4 % paraformaldehyde solution (PH7.4) for 2-4h at 4 ºC, and then blocks were cut from various parts of the lungs and airways for HE (light microscopy) and immunolight microscopy.

For immunolight microscopy, specimens were dehydrated through a graded series of alcohol, cleared and embedded in paraffin wax, and sectioned at 5 μm used for HE and immunohistochemical staining. Sections were dewaxed and rehydrated, an antigen retrieval procedure was performed to unmask antigens by treating the samples three times in a microwave oven at medium-high fire for 5 min each time in 10 mM citrate buffer, pH6. After cooling to room temperature, the sections were treated with 3 % hydrogen peroxide (H_2O_2) in distilled water for 30 min, then washed

three times with PBS for 10 min each. The sections were incubated in blocking reagent for 1 h and incubated overnight at 4°C with anti-AQP1diluted 1:200 (anti-AQP5) (Boster, Wuhan, China). The primary antibody was diluted in 10 mM PBS supplemented with 0.1 % BSA and 0.3 % Triton X-100 [10 mM PBS (7mM Na_2HPO_4, 3mM NaH_2PO_4, 150 mM NaCl, pH7.4)]. Subsequently, the sections were rinsed with 10 mM PBS for 3×10 min and incubated with biotinylated anti-rabbit IgG (ZSGB-BIO, Beijing, China, dilution: 1:200) secondary antibody for 2 h at room temperature. Then, the sections were rinsed with 10 mM PBS for 3×10 min and incubated with horseradish peroxidase streptavidin (ZSGB-BIO, Beijing, China, dilution: 1:200) tertiary antibody for 2 h at room temperature followed by coloration with diaminobenzidine (DAB; ZSGB-BIO, Beijing, China) for 30 s to visualize positive reaction. Counterstaining was with hematoxylin staining. The sections were carried out using bright microscopy (NI-V, Nikon, Japan).

Statistical analysis. Results of body weight measurements and lung function indexes were performed by unpaired t-test (two tailed). All data are presented as the mean ± SEM (standard error of the mean), **P*<0.05, ***P*<0.01.

RESULTS

Monthly measurement of body mass gain. Data on body mass of SD rats aged 8 weeks were no significant difference between normal group and smoke exposure groups before exposing. However, after three consecutive months of exposure to cigarette smoke, the body mass of rats in the normal group and 1st month, 2nd month and 3rd month smoke exposure group were respectively recorded, and monthly measurement of body mass gain were markedly difference compared with normal group (P<0.01) (Table I).

Table I. Monthly measurement of body mass gain after smoke exposure.

Cumulative exposure time	Mean ± SD (n=6)		*P*-value
	Control	Air pollutants exposure	
1st month	177.60±10.64	112.76±12.59	<0.01
2nd month	75.22±9.15	21.38±8.19	<0.01
3rd month	66.83±9.09	17.82±2.83	<0.01

Surface mucosa observation of nasal cavity. The surface of nasal cavity (including the turbinate and nasal septum region) and trachea of normal group and smoke exposure groups were showed by scanning electron micrographs (Fig. 1). Most of the surface on the turbinate region of normal group was covered with cilia, and goblet cells were evident (Fig. 1A). However, as the smoke exposure time accumulated, there were

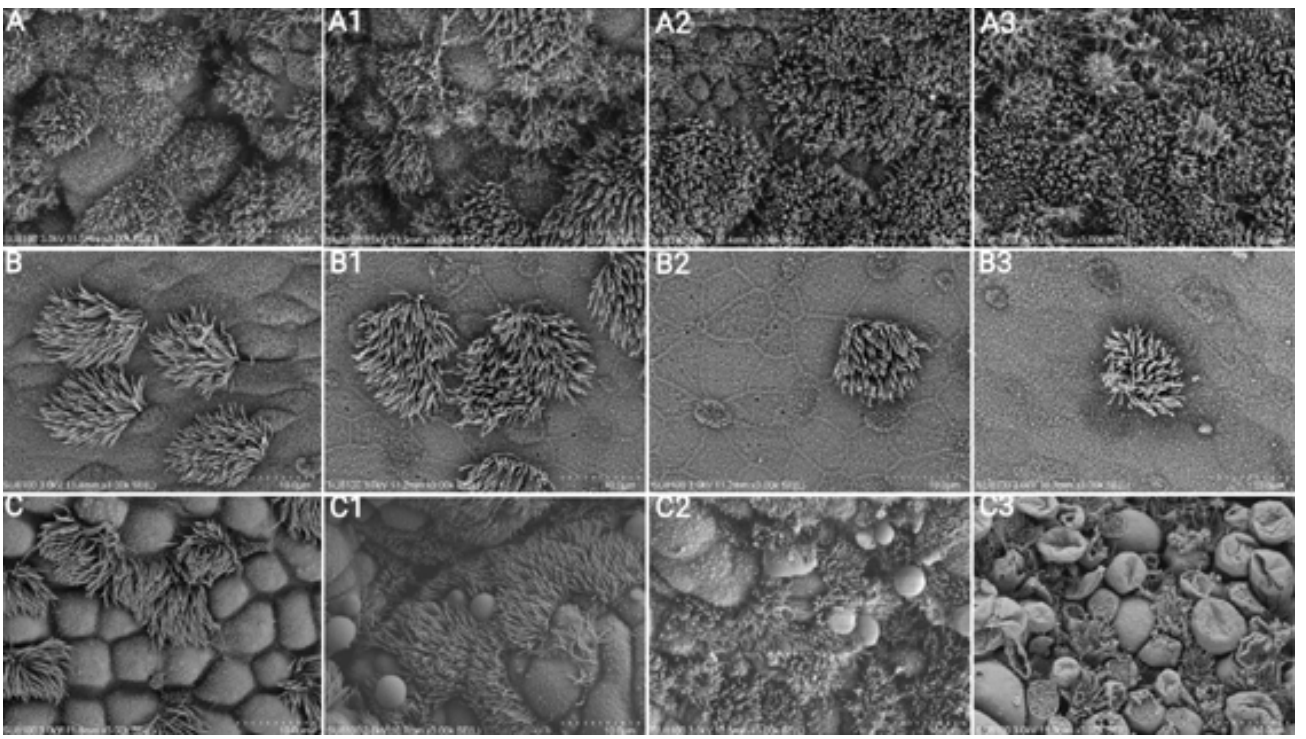

Fig.1. Observation of the surface of nasal cavity (including the turbinate and nasal septum region, A and B, respectively) and trachea (C) at normal group and smoke exposure groups (1st month, 2nd month and 3rd month smoke exposure group corresponding A1-A3, B1-B2,C1-C3, respectively) under scanning electron micrographs.

fewer and fewer goblet cells, and the cilia became more disorganized (Figs. 1A1-A3). And on nasal septum region, the morphology of cilia did not change much, but the number of cilia and goblet cells decreased significantly as compared with the normal group (Figs. 1B-B3).

Morphological structure observation of trachea. The mucous membrane of trachea of normal group was lined with typical respiratory epithelium by scanning electron micrographs. Ciliated columnar cells with well-developed cilia on the apical surface and numerous goblet cells were showed (Fig. 1C). However, with the accumulation of smoke exposure, there were obviously abnormal changes in the typical mucosal structure of the trachea of smoke exposure groups, particularly in the 3rd month smoke exposure group, a large number of goblet cells were collapsed and damaged, and cilia had become sparse and disorganized, or even broken (Figs. 2C1-C3).

Light microscopy of wall of the trachea in transverse section was showed by HE. The tracheal lumen was lined by respiratory epithelium (RE), a mixed seromucous gland (GL) in the submucosa drains to the epithelial surface via a small duct, hyaline cartilage (HC) surrounded by perichondrium is situated on the outer aspect of airway (Fig. 2A). However, for smoke exposure groups, the necrosis and exfoliation of epithelial cells can be uncovered in the mucosa, where pyknosis nucleus were hyperchromatic, fragmented or dissolved and disappeared. Moreover, the submucosa was mildly edematous, often with vascular congestion and dilation. And the connective tissue was loosely arranged, accompanied by a small amount of lymphocyte infiltration. Investigations by comparison on smoke exposure groups revealed this degree of pathological abnormality was positively correlated with the duration of smoke exposure by comparison (Figs. 2A1-A3).

Lung

Detection of lung function indexes. General lung function indexes of normal group and smoke exposure groups were measured by standard methods using Pulmonary Function Testing (DSI/BUXCO® PFT Controller, USA). Table II shows the results of general lung function indexes. PEF, MMEF and ERV were decreased in the 1st month smoke exposure group as compared with the normal group of rats ($P<0.05$). However, FRC, PEF, MMEF and ERV were decreased in the 2nd month smoke exposure group as compared with the normal group of rats ($P<0.05$ or $P<0.01$). In addition, all lung function indexes including FRC, FVC, IC, PEF, MMEF and ERV, were decreased in the 3rd month smoke exposure group as compared with the normal group ($P<0.05$ or $P<0.01$).

Morphological structure observation. Light microscopy of the lung in transverse section from normal group and smoke exposure groups were showed by HE. The bronchial

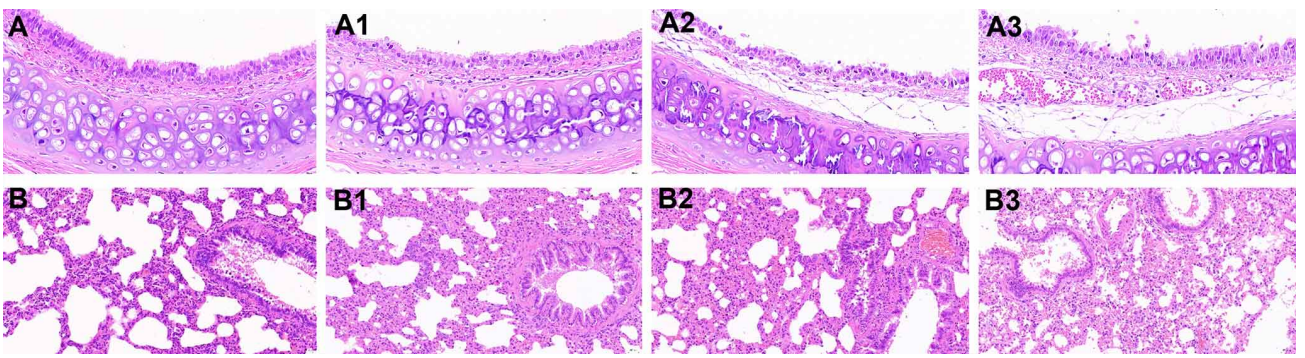

Fig. 2. Histologic structure of the trachea (A) and lung (B) at normal group and smoke exposure groups (1st month, 2nd month and 3rd month smoke exposure group corresponding A1-A3, B1-B2, respectively) in HE staining on paraffin section.

Table II. Lung function indexes of rats in control and smoke exposure group.

Items	1st month /Mean ± SD (n=6)		2nd month /Mean ± SD (n=6)		3rd month /Mean ± SD (n=6)	
	Control	Smoke exposure	Control	Smoke exposure	Control	Smoke exposure
FRC (ml)	12.94±1.07	12.12±1.45	13.66±0.79	10.82±0.92*	12.43±1.45	7.88±0.67**
FVC (ml)	25.94±1.37	24.47±0.91	25.99±1.66	24.20±1.33	26.72±1.40	22.92±1.85*
IC (ml)	22.21±1.52	20.58±1.30	21.72±1.60	20.45±0.95	21.87±1.38	17.84±1.36*
PEF (ml/s)	93.27±8.65	80.01±5.43*	87.63±7.55	59.54±7.35**	81.46±7.95	56.01±5.21**
MMEF (ml/s)	89.24±5.77	76.39±4.89*	85.62±4.31	57.17±3.18**	83.65±4.47	54.71±4.99**
ERV (ml)	5.61±0.59	4.62±0.65*	5.34±0.45	4.31±0.36*	5.16±0.46	3.67±0.43**

Note: FRC, Functional Residual Capacity; FVC, Forced Vital Capacity; IC, Inspiratory Capacity; PEF, Peak Expiratory Flow; MMEF, Maximal Mid-expiratory Flow; ERV, Expiratory Reserve Volume; Note: vs. control group, *P<0.05; **P<0.01.

epithelial cells were densely arranged, uniformly colored, and were normal in shape. Structurally, the alveolar wall was normal, like small pockets that were open on one side, similar to the honeycombs of a beehive. In addition, obvious hyperplasia, edema and inflammatory changes were no found in the normal group (Fig. 2B). However, the alveolar wall was moderately thickened in many places, the alveolar spacing was widened, and there was more granulocyte infiltration. Moreover, a small amount of bronchial epithelial cells were necrotic and exfoliated, and cell debris could be seen in the bronchial cavity. Due to local hemorrhage, red blood cells were seen in the bronchial cavity and in the surrounding alveolar cavity. In addition, mild edema around the blood vessels and loose arrangement of connective tissue were showed obviously, with a small amount of lymphocyte infiltration appearing in some areas of smoke exposure groups (Figs. 2B1-B3). It was showed as a whole that the extent of this histopathology increased with prolonged smoke exposure.

Transmission electron microscopy showed that the ultrastructure of the alveoli was normal as usual in the normal group, such as the intact alveolar wall and the continuous interalveolar septum. Meanwhile, the basement membranes (BM) were intact, continuous and uniform in thickness. Besides, Type I cells showed no edema, collagen fibers (CF) were abundant, and no large-scale hyperplasia (Fig. 3A).

However, for smoke exposure groups, part of the alveolar structure was damaged, such as alveolar collapse and fusion, and alveolar septum damage, in which a small amount of free flocculent protein can be seen. A large number of red blood cells (RBC) aggregated in the interstitial capillaries, and flocculent proteins were distributed in the

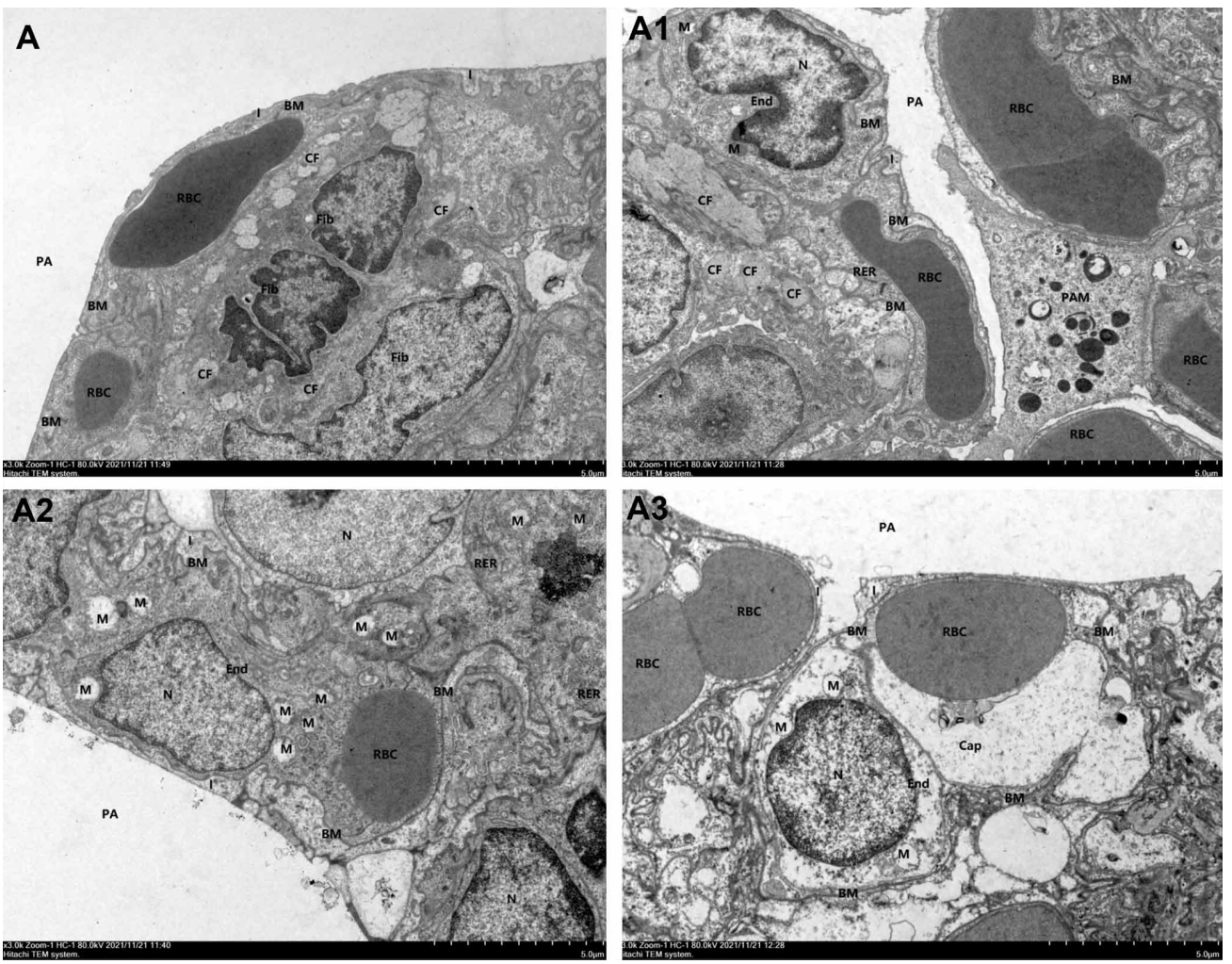

Fig. 3. Observation of blood-air barrier in the lung at normal group (A) and smoke exposure groups (1st month, 2nd month and 3rd month smoke exposure group corresponding A1-A3, respectively) with transmission electron microscope. PA, Pulmonary Alveolus; RBC, Red Blood Cell; BM, Basement Membrane; M, Mitochondria; N, Nucleus; CF, Collagenous fiber; I, Type I Alveolar Cell; End, Endotheliocyte; PAM, Pulmonary Macrophage, Fib, Fibroblast.

vascular lumens, but no obvious blockage was found. Endothelial cells (End) were severely edematous, and their nuclei (N) were irregularly shaped and bordered by heterochromatin. In addition, the number of mitochondria (M) was less, the membrane structure of mitochondrial was unclear, the cristae were reduced, and the matrix dissolved in a vacuolar shape. Besides, the BM was relatively intact, but the local structure was indistinct. Type I cells were markedly edematous (positively correlated with the duration of smoke exposure) (Figs. 3A1-A3).

AQPs protein examination. A deeper understanding of AQPs expression would provide useful information for lung pathophysiology and dysfunction, mainly including AQP1 and AQP5. Pronounced AQP1 immunohistochemical expression was detected in the endothelium of pulmonary capillary, vein and artery of normal group and smoke exposure groups at rats. Counterstaining with hematoxylin staining was used to identify negative segments (Fig. 4A). Whereas, for smoke exposure groups, weak labelling of AQP1 was clearly showed in the corresponding part of smoke exposure groups compared with normal group, respectively (Figs. 4A1-A3). Strong expression of AQP5 was localized in apical membrane of type I cells of the alveolar epithelium of normal group (Fig. 4B). However, for smoke exposure groups, weak labelling of AQP5 was clearly detected in the corresponding part of smoke exposure groups compared with normal group, respectively (Figs. 4B1-B3).

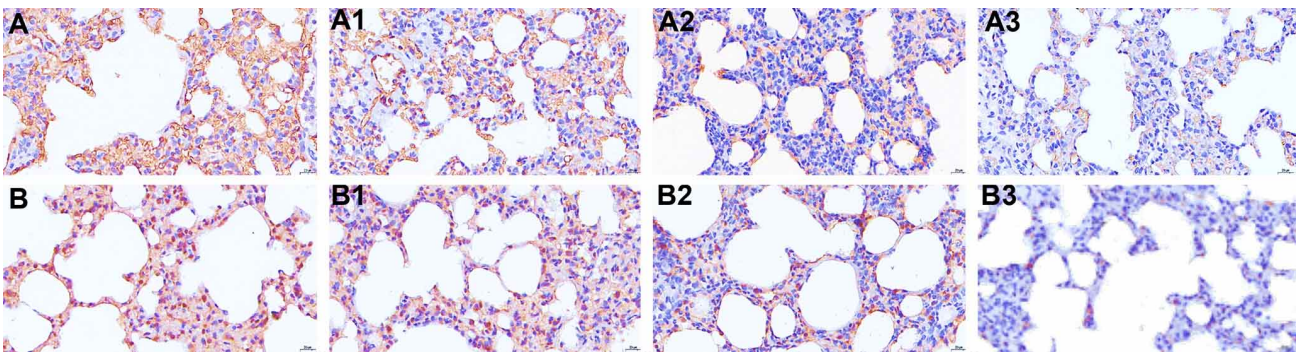

Fig. 4. Immunohistochemical examination of AQP1 (A) and AQP5 (B) protein abundance in the lung at tissue section from normal group and smoke exposure groups (1st month, 2nd month and 3rd month smoke exposure group corresponding A1-A3, B1-B2, respectively).

DISCUSSION

Public awareness of the detrimental effects of air pollution on respiratory health is increasing, particularly in relation to haze days in daily, and remains a major global public health threat. As we all know, respiratory system includes two main functions of ventilation and oxygenation, and the corresponding functional structures are the airways and pulmonary alveoli, respectively. Before the inspired air enters the alveoli, it should be cleansed firstly. To carry out this function, the mucosa of airways is lined with a specialized respiratory epithelium, and there are well-developed cilia and numerous mucous/serous glands (Wanner, 1986). In a word, these structures are necessary and together carry out so-called mucociliary clearance.

In this study, firstly we observed the data on monthly measurement of body mass gain were markedly difference compared with normal group, and it was decreased overall with prolonged smoke exposure. In addition, lung function indexes including FRC, FVC, IC, PEF, MMEF and ERV, were decreased to some extent, especially in the 3rd month smoke exposure group. Therefore, it hinted the abnormal changes on body mass and lung function indexes may reflect suboptimal body functioning.

Normal Cilia, which are cylindrical projections from the apical surface of the mucosal columnar epithelial cells, are complex structures of airways in which its function is critical to respiratory defense. Cilia beat in a coordinated manner to clear upper airway of the mucus blanket that are continually inspired in normal respiration (Houtmeyers *et al*., 1999; Satir & Sleigh, 1990). Mucus produced by goblet cells interspersed on the apical surface of epithelial cells have a tremendous effects on mucociliary clearance (Houtmeyers *et al*., 1999). Certainly, the structure of mucus itself is also altered by disease states, such as cigarette smoke (Kreindler *et al*., 2005; Cohen *et al*., 2009). In this study, as the smoke exposure time accumulated, there were fewer and fewer normal goblet cells, and the cilia became more disorganized in the nasal cavity andtrachea. Additionally, the number of normal cilia and goblet cells decreased significantly as compared with the normal group. In cystic fibrosis (CF), dysfunctional chloride transport secondary to a mutation of

the gene for the protein CF transmembrane conductance regulator results in abnormal mucus and severe mucociliary dysfunction (Hegab *et al*., 2007; Virgin *et al*., 2010). Therefore, it is suggested that these pathological findings may explain why smoke exposure groups show airway histopathology similar to that of CF patients, most likely via disruptions in mucosal ion transport (Gudis *et al*., 2012).

Previous studies have demonstrated that it is critical to keep fluid balance in respiratory tract and alveolus epithelium to maintain normal respiratory function. Resorptive and secretory fluid transport across epithelium must be kept in a range that guarantees an appropriate gas exchange and other functions, such as mucociliary clearance (Song *et al*., 2017; Wittekindt & Dietl, 2019). AQPs are water channel proteins supposed to facilitating fluid transport in airway humidification, submucosal gland secretion and alveolar space, including AQP1, AQP3, AQP4 and AQP5 (Yasui *et al*., 1997; Nielsen *et al*., 1997; Funaki *et al*., 1998; Kreda *et al*., 2001; Krane *et al*., 2001; Maeda *et al*., 2005; Schmidt *et al*., 2017).

The lining liquid of respiratory tract and alveoli, also denoted airway or alveolar surface liquid (ASL), has several functions in the previous studies, such as protection, mucociliary clearance (Ravasio *et al*., 2011; Wine *et al*., 2018). ASL formation and stabilization both depend on fluid secretion and resorption, as a result of active ion transport. Therefore, it was consistent as we just have discussed that smoke exposure groups show airway histopathology similar to that of CF patients, most likely via disruptions in mucosal ion transport.

In addition, beside certain osmotic gradients, hydrostatic pressure gradients across endothelial/epithelial barrier can also force water to move from the vascular lumen onto the apical surface of the lung epithelium. Even though the pathways for transepithelial ion transport across pulmonary epithelia are well established, the pathways for water flux remained elusive, especially fluid transport via AQPs in the lung (Wittekindt & Dietl, 2019). AQP1 is reported to be localized in plasma membranes of endothelial cells that form the barrier of blood vessels along the airways as well as within the respiratory and alveolar regions (Towne *et al*., 2000; Maeda *et al*., 2005; Dong *et al*., 2012; Wu *et al*., 2015). AQP5 is detected in the apical membrane of cuboidal cells along respiratory bronchiole and in alveolar epithelial type ? cells (Jiang *et al*., 2015; Kreda *et al*., 2001; Dong *et al*., 2012; Fabregat *et al*., 2014).

Generally, water that covers the surface of airways and alveoli originates in the vascular compartment, from where it has to pass two barriers in series into the airspace via AQPs-mediated transendothelial/transepithelial water flux. Studies in lungs of AQPs knockout animals demonstrate that both AQP1 and AQP5 mediated the dominating route for water flux across the pulmonary microvascular endothelium (Ma *et al*., 2000; King *et al*., 2002). In this study, compared with normal group, weak labelling of AQP1 and AQP5 were clearly detected in the corresponding part of smoke exposure groups compared with normal group, respectively. In addition, evidences from reports on lung diseases that AQPs are involved especially in those diseases that are caused or accompanied by perturbed balancing resorptive and secretory fluid homeostasis, such as asthma, chronic obstructive pulmonary disease and acute lung injury (Wang *et al*., 2007; Shen *et al*., 2012; Zhao *et al*., 2014; Zhang *et al*., 2015; Tao *et al*., 2016). Based on the result of reducing protein abundance for AQP1 and AQP5 in the smoke exposure groups in this study, therefore, it is suggested that the contribution of AQPs to transendothelial and transepithelial water permeability (namely near-isosmolar fluid homeostasis) is diminished, thereby affecting the normal balancing resorptive and secretory fluid transport.

Taken together, the formation and stabilization of ASL is at least involved osmotic gradients and endothelial/epithelial barrier, the former is a result of active ion transport, while the latter depends on AQPs-mediated transendothelial/transepithelial transport. At least, general down-regulation of AQPs protein abundance in the lung of smoke exposure suggests that ASL is abnormal balance, especially in the endothelial/epithelial barrier. Certainly, whether there is a compensation mechanism from osmotically pressure is unknown so far. To further understand the pivotal role for water transport in the lung, it maybe needs a more detailed analysis and further investigation, despite its difficult experimental and technical accessibility.

Long-term exposure to cigarette smoke, adverse changes of form and function may develop in the lining of airways and alveolar, for example, mucus production is increased, ciliary function is depressed, mucosal characteristics are altered and so on. More importantly, the function of AQPs-mediated transendothelial and transepithelial water flux is diminished, thereby affecting ASL formation and stabilization in some extent. It also was reported that IL-13 transiently downregulated AQP5 mRNA levels in asthma with inflammatory process of the airways (Krane *et al*., 2009; Dong *et al*., 2012; Rana *et al*., 2016). Therefore, additional studies on IL-13 would be required to study the signaling cascades involved overall down-regulation of AQPs whereby exposure to cigarette smoke. Furthermore, even when these basic issues are well understood, it will still be a great challenge to elucidate the exact role of AQPs in lung physiological and pathophysiological processes under special conditions and disease.

ACKNOWLEDGMENTS

We thank Yanli Lei and Xiaoya Mai (Undergraduates) for assistance with sample collection in this study. This work was supported by the Natural Science Fund of Ningxia (2020AAC03167) and Innovation and Entrepreneurship Training Program for Undergraduates of Ningxia Medical University (S202110752051), China.

WANG, J.; DING, R.; LIANG, J.; WANG, H. & WANG, P. Efectos morfológicos del consumo de cigarrillos en el sistema respiratorio y funciones relacionadas según la expresión de AQP. *Int. J. Morphol., 41(2)*:539-547, 2023.

RESUMEN: Cada vez se presta más atención a la contaminación del aire en la salud respiratoria, particularmente, en relación con los días de neblina. En consecuencia la exposición al humo del cigarrillo aumenta la toxicidad de los contaminantes comunes del aire, lo que además aumenta la complejidad de las enfermedades respiratorias. Aunque existen varios mecanismos involucrados en las enfermedades respiratorias causadas o empeoradas por el tabaquismo, en las que el papel de las AQP en el pulmón respecto a la homeostasis de líquidos sigue siendo difícil de alcanzar. En este artículo, copiamos los modelos de rata basados en el generador de humo e investigamos los cambios morfológicos de la mucosa y las funciones relacionadas según el equilibrio del líquido de revestimiento de los alvéolos a través de la expresión de AQP. En comparación con el grupo normal, se detectó claramente un etiquetado débil de la abundancia de proteínas AQP1 y AQP5 en la parte correspondiente de los grupos de exposición al humo en comparación con el grupo control. Por lo tanto, se sugiere que la contribución de las AQP en el pulmón está disminuida, provocando así un equilibrio perturbado entre la homeostasis del líquido secretor y de reabsorción bajo el hábito de fumar cigarrillos.

PALABRAS CLAVE: Sistema respiratorio; Fumar cigarrillos; Patomorfología; Acuaporinas (AQP); Homeostasis de fluidos.

REFERENCES

Cohen, N. A.; Zhang, S.; Sharp, D. B.; Tamashiro, E.; Chen, B.; Sorscher, E. J. & Woodworth, B. A. Cigarette smoke condensate inhibits transepithelial chloride transport and ciliary beat frequency. *Laryngoscope, 119(11)*:2269-74, 2009.

Dong, C.; Wang, G.; Li, B.; Xiao, K.; Ma, Z.; Huang, H.; Wang, X. & Bai, C. Anti-asthmatic agents alleviate pulmonary edema by upregulating AQP1 and AQP5 expression inthe lungs of mice with OVA-induced asthma. *Respir. Physiol. Neurobiol., 181(1)*:21-8, 2012.

Fabregat, G.; García-de-la-Asunción, J.; Sarriá, B.; Cortijo, J.; De Andrés, J.; Mata, M.; Pastor, E. & Belda, F. J. Increased expression of AQP 1 and AQP 5 in rat lungs ventilated with low tidal volume is time dependent. *PloS One, 9(12)*:e114247, 2014.

Folkesson, H. G.; Matthay, M. A.; Hasegawa, H.; Kheradmand, F. & Verkman, A. S. Transcellular water transport in lung alveolar epithelium through mercury-sensitive waterchannels. *Proc. Natl. Acad. Sci. U. S. A., 91(11)*:4970-4, 1994.

Funaki, H.; Yamamoto, T.; Koyama, Y.; Kondo, D.; Yaoita, E.; Kawasaki, K.; Kobayashi, H.; Sawaguchi, S.; Abe, H. & Kihara, I. Localization and expression of AQP5 in cornea, serous salivary glands, and pulmonary epithelial cells. *Am. J. Physiol., 275(4)*:C1151-7, 1998.

Gudis, D.; Zhao, K. Q. & Cohen, N. A. Acquired cilia dysfunction in chronic rhinosinusitis. *Am. J. Rhinol. Allergy., 26(1)*:1-6, 2012.

Hegab, A. E.; Sakamoto, T.; Nomura, A.; Ishii, Y.; Morishima, Y.; Iizuka, T.; Kiwamoto, T.; Matsuno, Y.; Homma, S. & Sekizawa, K. Niflumic acid and AG-1478 reduce cigarette smoke-induced mucin synthesis: the role of hCLCA1. *Chest, 131(4)*:1149-56, 2007.

Houtmeyers, E.; Gosselink, R.; Gayan-Ramirez, G. & Decramer, M. Regulation of mucociliary clearance in health and disease. *Eur. Respir. J., 13(5)*:1177-88, 1999.

Jiang, Y. X.; Dai, Z. L.; Zhang, X. P.; Zhao, W.; Huang, Q. & Gao, L. K. Dexmedetomidine alleviates pulmonary edema by upregulating AQP1 and AQP5 expression in rats with acute lung injury induced by lipopolysaccharide. *J. Huazhong Univ. Sci. Technolog. Med. Sci., 35(5)*:684-8, 2015.

King, L. S.; Nielsen, S.; Agre, P. & Brown, R. H. Decreased pulmonary vascular permeability in aquaporin-1-null humans. *Proc. Natl. Acad. Sci. U. S. A., 99(2)*:1059-63, 2002.

Krane, C. M. & Goldstein, D. L. Comparative functional analysis of aquaporins/glyceroporins in mammals and anurans. *Mamm. Genome, 18(6-7)*:452-62, 2007.

Krane, C. M.; Deng, B.; Mutyam, V.; McDonald, C. A.; Pazdziorko, S.; Mason, L.; Goldman, S.; Kasaian, M.; Chaudhary, D.; Williams, C.; *et al*. Altered regulation of aquaporin gene expression in allergen and IL-13-induced mouse models of asthma. *Cytokine, 46(1)*:111-8, 2009.

Krane, C. M.; Fortner, C. N.; Hand, A. R.; McGraw, D. W.; Lorenz, J. N.; Wert, S. E.; Towne, J. E.; Paul, R. J.; Whitsett, J. A. & Menon, A. G. Aquaporin 5-deficient mouse lungs are hyperresponsive to cholinergic stimulation. *Proc. Natl. Acad. Sci. U. S. A., 98(24)*:14114-9, 2001.

Kreda, S. M.; Gynn, M. C.; Fenstermacher, D. A.; Boucher, R. C. & Gabriel, S. E. Expression and localization of epithelial aquaporins in the adult human lung. *Am. J. Respir. Cell. Mol. Biol., 24(3)*:224-34, 2001.

Kreindler, J. L.; Jackson, A. D.; Kemp, P. A.; Bridges, R. J. & Danahay, H. Inhibition of chloride secretion in human bronchial epithelial cells by cigarette smoke extract. *Am. J. Physiol. Lung Cell. Mol. Physiol., 288(5)*:L894-L902, 2005.

Ma, T.; Fukuda, N.; Song, Y.; Matthay, M. A. & Verkman, A. S. Lung fluid transport in aquaporin-5 knockout mice. *J. Clin. Invest., 105(1)*:93-100, 2000.

Maeda, S.; Ito, H.; Tanaka, K.; Hayakawa, T. & Seki, M. Localization of aquaporin water channels in the airway of the musk shrew (*Suncus murinus*) and the rat. *J. Vet. Med. Sci., 67(10)*:975-84, 2005.

Nielsen, S.; King, L. S.; Christensen, B. M. & Agre, P. Aquaporins in complex tissues. II. Subcellular distribution in respiratory and glandular tissues of rat. *Am. J. Physiol., 273(5)*:C1549-61, 1997.

Nielsen, S.; Smith, B. L.; Christensen, E. I. & Agre, P. Distribution of the aquaporin CHIP in secretory and resorptive epithelia and capillary endothelia. *Proc. Natl. Acad. Sci. U. S. A., 90(15)*:7275-79, 1993.

Rana, S.; Shahzad, M. & Shabbir, A. Pistacia integerrima ameliorates airway inflammation by attenuation of TNF-a, IL-4, and IL-5 expression levels, and pulmonary edema by elevation of AQP1 and AQP5 expression levels in mouse model of ovalbumin-induced allergic asthma. *Phytomedicine, 23(8)*:838-45, 2016.

Ravasio, A.; Hobi, N.; Bertocchi, C.; Jesacher, A.; Dietl, P. & Haller, T. Interfacial sensing by alveolar type II cells: a new concept in lung physiology? *Am. J. Physiol. Cell. Physiol., 300(6)*:C1456-65, 2011.

Satir, P. & Sleigh, M. A. The physiology of cilia and mucociliary interactions. *Annu. Rev. Physiol., 52*:137-55, 1990.

Sato, S. & Kiyono, H. The mucosal immune system of the respiratory tract. *Curr. Opin. Virol., 2(3)*:225-32, 2012.

Schmidt, H.; Michel, C.; Braubach, P.; Fauler, M.; Neubauer, D.; Thompson, K. E.; Frick, M.; Mizaikoff, B.; Dietl, P. & Wittekindt, O. H. Water permeability adjusts resorption in lung epithelia to increased apical surface liquid volumes. *Am. J. Respir. Cell Mol. Biol., 56(3)*:372-82, 2017.

Shen, Y.; Wang, X.; Wang, Y.; Wang, X.; Chen, Z.; Jin, M. & Bai, C. Lipopolysaccharide decreases aquaporin 5, but not aquaporin 3 or aquaporin 4, expression in human primary bronchial epithelial cells. *Respirology, 17(7)*:1144-9, 2012.

Song, Y.; Wang, L.; Wang, J. & Bai, C. Aquaporins in respiratory system. *Adv. Exp. Med. Biol., 969*:115-22, 2017.

Tao, B.; Liu, L.; Wang, N.; Wang, W.; Jiang, J. & Zhang, J. Effects of hydrogen-rich saline on aquaporin 1, 5 in septic rat lungs. *J. Surg. Res., 202(2)*:291-8, 2016.

Towne, J. E.; Harrod, K. S.; Krane, C. M. & Menon, A. G. Decreased expression of aquaporin (AQP)1 and AQP5 in mouse lung after acute viral infection. *Am. J. Respir. Cell Mol. Biol., 22(1)*:34-4, 2000.

Tsukita, S.; Yamazaki, Y.; Katsuno, T.; Tamura, A. & Tsukita, S. Tight junction-based epithelial microenvironment and cell proliferation. *Oncogene, 27(55)*:6930-8, 2008.

Virgin, F. W.; Azbell, C.; Schuster, D.; Sunde, J.; Zhang, S.; Sorscher, E. J. & Woodworth, B. A. Exposure to cigarette smoke condensate reduces calcium activated chloride channel transport in primary sinonasal epithelial cultures. *Laryngoscope, 120(7)*:1465-9, 2010.

Wang, K.; Feng, Y. L.; Wen, F. Q.; Chen, X. R.; Ou, X. M.; Xu, D.; Yang, J. & Deng, Z. P. Decreased expression of human aquaporin-5 correlated with mucus overproductionin airways of chronic obstructive pulmonary disease. *Acta. Pharmacol. Sin., 28(8)*:1166-74, 2007.

Wanner, A. Mucociliary clearance in the trachea. *Clin. Chest Med., 7(2)*:247-58,1986.

Wine, J. J.; Hansson, G. C.; König, P.; Joo, N. S.; Ermund, A. & Pieper, M. Progress in understanding mucus abnormalities in cystic fibrosis airways. *J. Cyst. Fibros., 17(2S)*:S35-9, 2018.

Wittekindt, O. H. & Dietl, P. Aquaporins in the lung. *Pflugers. Arch., 471(4)*:519-32, 2019.

Wu, Y.; Pan, C. Y.; Guo, C. Z.; Dong, Z. J.; Wu, Q.; Dong, H. M. & Zhang, W. Expression of aquaporin 1 and 4 in rats with acute hypoxic lung injury and its significance. *Genet. Mol. Res., 14(4)*:12756-64, 2015.

Yasui, M.; Serlachius, E.; Löfgren, M.; Belusa, R.; Nielsen, S. & Aperia, A. Perinatal changes in expression of aquaporin-4 and other water and ion transporters in rat lung. *J. Physiol., 505(1)*:3-11, 1997.

Yonemura S. Cadherin-actin interactions at adherens junctions. *Curr. Opin. Cell Biol., 23(5)*:515-22, 2011.

Zhang, J.; Gong, L.; Hasan, B.; Wang, J.; Luo, J.; Ma, H. & Li, F. Use of aquaporins 1 and 5 levels as a diagnostic marker in mild-to-moderate adult-onset asthma. *Int. J. Clin. Exp. Pathol., 8(11)*:14206-13, 2015.

Zhao, R.; Liang, X.; Zhao, M.; Liu, S. L.; Huang, Y.; Idell, S.; Li, X. & Ji, H. L. Correlation of apical fluid-regulating channel proteins with lung function in human COPD lungs. *PloS One, 9(10)*:e109725, 2014.

Corresponding author:
Jinbao Wang
School of Basic Medicine
Ningxia Medical University
Yinchuan
750004 Ningxia
CHINA

E-mail: wangjinbao123asd@126.com